Lab on a Chip

PAPER

View Article Online
View Journal | View Issue

Cite this: *Lab Chip*, 2022, **22**, 1815

Emulating the chondrocyte microenvironment using multi-directional mechanical stimulation in a cartilage-on-chip†

Carlo Alberto Paggi,[ab] Jan Hendriks,[a] Marcel Karperien *[a] and Séverine Le Gac *[b]

The multi-directional mechanical stimulation experienced by articular cartilage during motion is transferred to the chondrocytes through a thin layer of pericellular matrix around each cell; chondrocytes in turn respond by releasing matrix proteins and/or matrix-degrading enzymes. In the present study we investigated how different types of mechanical stimulation can affect a chondrocyte's phenotype and extracellular matrix (ECM) production. To this end, we employed a cartilage-on-chip system which allows exerting well-defined compressive and multi-directional mechanical stimulation on a 3D chondrocyte-laden agarose hydrogel using a thin deformable membrane and three individually addressed actuation chambers. First, the 3D chondrocyte culture in agarose responded to exposure to mechanical stimulation by an initial increase in IL-6 production and little-to-no change in IL-1β and TNF-α secretion after one day of on-chip culture. Exposure to mechanical stimulation enhanced *COL2A1* (hyaline cartilage marker) and decreased *COL1A1* (fibrotic cartilage) expression, this being more marked for the multi-directional stimulation. Remarkably, the production of glycosaminoglycans (GAGs), one of the main components of native cartilage ECM, was significantly increased after 15 days of on-chip culture and 14 days of mechanical stimulation. Specifically, a thin pericellular matrix shell (1–5 μm) surrounding the chondrocytes as well as an interstitial matrix, both reminiscent of the *in vivo* situation, were deposited. Matrix deposition was highest in chips exposed to multi-directional mechanical stimulation. Finally, exposure to mechanical cues enhanced the production of essential cartilage ECM markers, such as aggrecan, collagen II and collagen VI, a marker for the pericellular matrix. Altogether our results highlight the importance of mechanical cues, and using the right type of stimulation, to emulate *in vitro*, the chondrocyte microenvironment.

Received 26th November 2021,
Accepted 22nd March 2022

DOI: 10.1039/d1lc01069g

rsc.li/loc

Introduction

Mechanical stimulation of chondrocytes is essential for keeping joints healthy. Upon movement, signals generated by the load induce homeostatic regulators that support the re-organization and maintenance of the cartilaginous extracellular matrix (ECM).[1] Prolonged immobilization of joints leads to atrophy, a condition in which chondrocytes become quiescent resulting in a net cartilage mass loss through ECM degradation.[2] The influence of mechanical stimulation in the development of disease conditions, such as osteoarthritis (OA) and rheumatoid arthritis (RA), is recognized globally and has been extensively reviewed.[3,4] For instance, direct (joint articular fractures) and indirect (joint destabilization due to ligament or meniscus rupture) injuries enhance the risk of OA development due to a change in the mechanical stimulation pattern of the chondrocytes.[5] Furthermore, other factors such as obesity and abnormal gait, in which knee cartilage is exposed to hyper-physiological loads, are considered as OA inducers.[6]

Articular cartilage in the knee joint is a complex tissue acting as a protective layer for the underlying bones during movement. This hyaline cartilage does not comprise any blood vessels or nerves making mechanical stimulation one of the main mediators for intercellular communication by facilitating diffusion of signaling molecules and nutrients by load-induced extracellular fluid flow.[7] The articular cartilage structure can roughly be divided into two main elements, the interstitial matrix and the pericellular matrix. First, the bulk or interstitial

[a] *Department of Developmental BioEngineering, TechMed Centre, and Organ-on-chip Centre, University of Twente, Enschede, The Netherlands. E-mail: marcel.karperien@utwente.nl*
[b] *Applied Microfluidics for BioEngineering Research, MESA+ Institute for Nanotechnology & TechMed Centre, and Organ-on-chip Centre, University of Twente, Enschede, The Netherlands. E-mail: s.legac@utwente.nl*
† Electronic supplementary information (ESI) available. See DOI: https://doi.org/10.1039/d1lc01069g

matrix is rich in proteoglycans such as aggrecan and collagen II fibers running parallel to the surface in the superficial layers, shifting to perpendicular organization in the middle and deep zones of this tissue. This interstitial matrix absorbs most of the compressive and sliding forces exerted during joint movement.[8] Next, the chondrocytes are surrounded by a much softer pericellular matrix. This pericellular matrix, which protects the chondrocytes from forces experienced by the interstitial matrix, is a 1–5 μm thick layer, which is rich in collagen VI, aggrecan and collagen II.[9] During movement, the load is transmitted from the bulk matrix to the pericellular matrix, and chondrocytes, which sense ECM structural modifications, progressively respond to those by altering their matrix protein and matrix-degrading enzyme production.[10]

In the last decades, *in vitro* models have been reported to study – and possibly reproduce – the pericellular matrix and characterize chondrocyte organization in cartilage.[11] For instance, growth factors added to the culture medium in 3D static culture or in cartilage repair promote the pericellular matrix formation as reviewed elsewhere.[12] However, chondrocytes in the articular cartilage *in vivo* experience well-defined mechanical stimuli, which current static *in vitro* models lack, while they are likely to be key to generate a quasi-native pericellular matrix in a relatively short time. To explore the impact of this mechanical component, organ-on-a-chip (OoC) models of cartilage have been developed, that all integrate a mechanical actuation unit. For instance, Occhetta *et al.* reported homogeneous compression of a 3D hydrogel loaded with human chondrocytes using a horizontal deformable polydimethylsiloxane (PDMS) membrane placed below the cell-hydrogel constructs; they successfully exerted both physiological and hyper-physiological stimulation to trigger an inflammatory state as found in OA.[13] Rosser *et al.* cultured equine chondrocytes in a hydrogel matrix in a microfluidic device, with continuous delivery of nutrients and possibly inflammatory cytokines in a channel adjacent to the 3D cell-hydrogel construct, to create an OA model. The fluid shear stress experienced by cartilage upon loading was emulated with flow applied in the device.[14] Yet, these two examples only include one type of mechanical stimulation, while articular cartilage experiences multi-directional stimulation,[15] which is known to affect the chondrocyte matrix protein production and matrix 3D architecture.[16] More specifically, chondrocytes are exposed to different levels of compression and shear strain simultaneously, also depending on their specific position within the cartilage: close to the surface, chondrocytes feel both compressive and shear strain, while in the deeper layer stimulation is mainly compressive. In previous work, we developed a cartilage-on-chip platform able to generate both compressive and multi-directional mechanical stimulation on cell-laden hydrogels, and healthy and/or hyper-physiological loading as experienced by the joint during movement.[17] Yet, we did not study how the different mechanical stimulation modalities could influence the chondrocyte phenotype, function, and their microenvironment.

Here, we wanted to highlight the effect of different biomechanical stimuli on the chondrocyte protein production. Hence, we further characterize the response of human chondrocytes to multi-directional mechanical stimulation in our cartilage-on-chip platform and examine if such stimulation could aid in the generation of quasi-native articular matrix. After small adaptations in the design of the platform to improve its performance, we examined the secretory profile (IL-6, IL-1β and TNF-α inflammatory markers) of chondrocytes upon their introduction in the cartilage-on-chip platform and exposure to mechanical stimulation (compression only & multi-directional mechanical stimulation (mdms)). Following this, we quantified differences in mRNA expression levels for *COL1A1*, *COL2A1*, *SOX9*, *COL10A1*, and *KI67* for static, compression only and multi-directional stimulation conditions. Next, we examined glycosaminoglycan (GAG) production for the same three conditions in terms of creation of a pericellular matrix around individual human chondrocytes and interstitial matrix deposition. Lastly, we determined the chondrocyte production in aggrecan, collagen II and collagen VI, which are three of the main markers of hyaline cartilage. Collectively, our results highlight the importance of applying proper mechanical stimulation for the physiological regulation of chondrocytes and emulating their microenvironment through the production of native pericellular matrix.

Materials and methods

Cell culture

Human chondrocytes were isolated from histologically healthy-looking cartilage from patients undergoing total knee replacement.[18] The collection and use of human cartilage was approved by a medical ethical committee (METC) of Zorggroep Twente, The Netherlands. Human chondrocytes were cultured in T175 flasks (Cellstar®, Greiner bio-one, Germany) in chondrocyte proliferation medium (DMEM with 10% FBS (fetal bovine serum), 0.2 mM ascorbic acid 2-phosphate, 0.1 mM non-essential amino acids, 100 U ml^{-1} penicillin and 100 μg ml^{-1} streptomycin, 4 mM proline).[19,20] Cells were passaged using a trypsin–EDTA (1×) solution (0.25%/0.1 mM, respectively, Invitrogen, Carlsbad, CA, USA) in PBS and re-seeded in a new flask at a concentration of 500 000 cells per 175 cm^2. Cells were used at passage 4 for all experiments reported in this paper.

Microfluidic device fabrication

The cartilage-on-chip devices were produced using soft-lithography from PDMS and using a SU-8-on-silicon mould previously fabricated in the Nanolab cleanrooms of the MESA+ Institute for Nanotechnology, as previously described.[17] Briefly, designs were drawn using Clewin (WieWeb software, Hengelo, The Netherlands), from which a mask was produced (DeltaMask, Enschede, The Netherlands). SU-8100 photoresist (MicroChem, Westborough, MA, USA) was spin-coated on a <100> silicon wafer (Okmetic, Vantaa, Finland) with a final thickness of 250 μm. After a first baking step, the SU-8 layer was patterned by photolithography, next baked and developed according to the manufacturer's specification. A mixture of PDMS pre-polymer and curing agent (Sylgard 184, Dow Corning,

Midland, MI, USA) with a weight ratio of 20 : 1 was poured on the mould and cured at 60 °C for 24 h. 1 and 2 mm diameter punchers were used to create inlets and outlets of the device. A 4 mm thick PDMS layer was prepared in the same manner as the microfluidic layer on a dummy wafer and bonded to a glass slide.[17] The microfluidic layer was finally assembled to this PDMS-coated glass substrate (Fig. 1). Both bonding steps were performed using plasma treatment (Cute, Femto Science, Gyeonggi-do, South Korea). The final cartilage-on-a-chip devices were placed in an oven at 60 °C for 24 h before use.

Membrane and hydrogel deformation under compression

The PDMS membrane deformation in the upgraded cartilage-on-chip device was first characterized by applying homogeneous compression, which was achieved by applying the same positive pressure in the three actuation chambers, as previously reported.[17] Pressure was generated using a positive pressure controller (MFCS-EZ, pressure output from 0 to 2000 mbar, Fluigent, Le Kremlin-Bicêtre, France), and Microfluidic Automation tool software (AiO-All in One) (Fluigent). Hydrogel deformation was next examined by supplementing low melting temperature agarose 2% w/v (low melting temperature agarose, Invitrogen) in PBS with 15 μm diameter polystyrene microbeads (60 μg ml^{-1}, Kisker-Biotech, Steinfurt, Germany). For homogeneous compression, the bead displacement normal to the membrane was quantified as a function of their distance from the membrane. Here, only microbeads located in front of the middle actuation chamber were considered in this analysis.

Cell culture in the cartilage-on-chip platform

Low melting temperature agarose 2% w/v supplemented with 1 500 000 cells per ml was injected in the culture chamber in

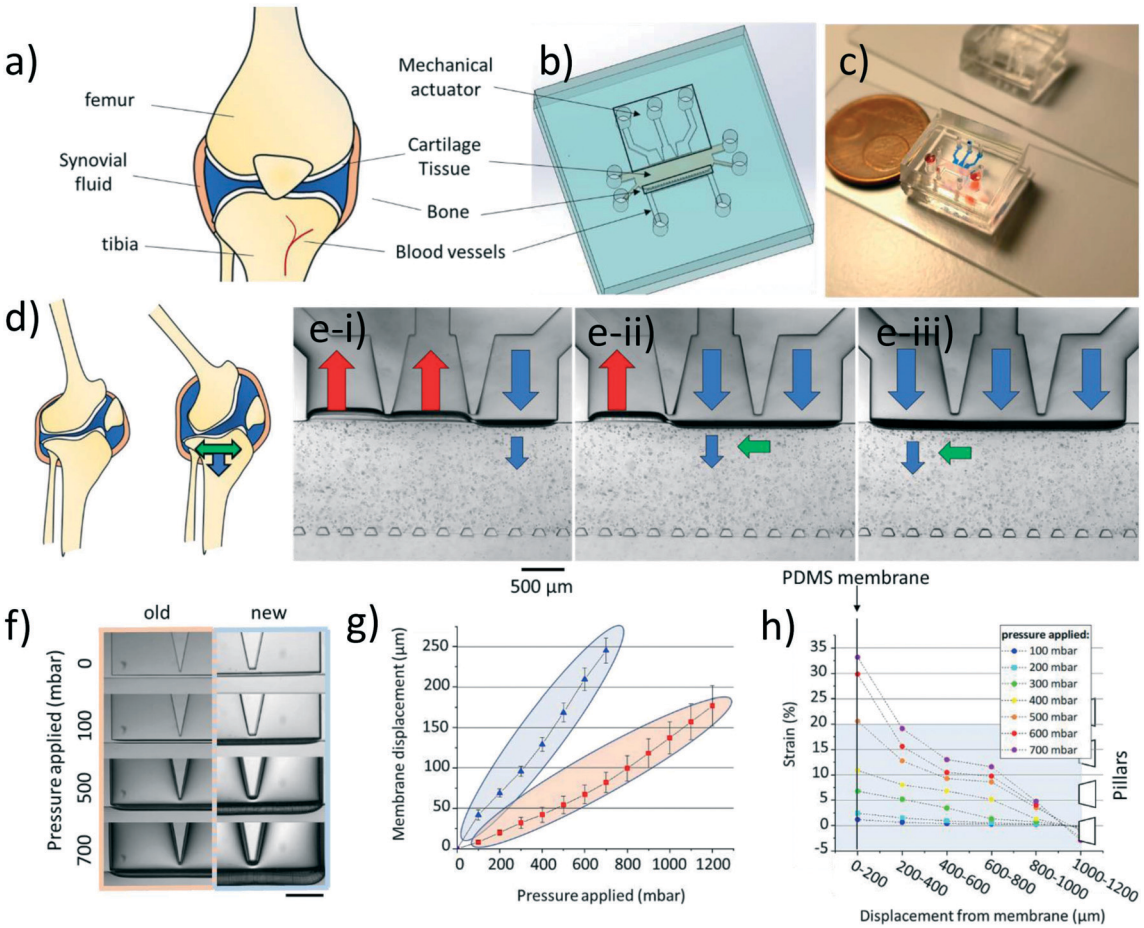

Fig. 1 Cartilage-on-chip design, operation, and characterization. a) Schematic representation of the knee joint. b) Design of the cartilage-on-chip device, highlighting its main features. c) Top view of the cartilage-on-chip device filled in with food dyes for visualization purposes – actuation unit in blue; cell-hydrogel chamber in red and perfusion channel in yellow. d) Side-view schematic of the joint during motion, depicting the generated multi-directional mechanical stimulation (shear strain – green arrow & compression – blue arrow). e i–iii) Top view of the cartilage-on-chip device filled in with human chondrocytes in agarose exposed to a sequence generating multi-directional mechanical stimulation, as detailed in the text: blue arrows depict compression and green arrows shear strain. Scale bar = 500 μm. f) Top view of the device comparing the membrane deformation in the previous and upgraded platforms at different pressures (0, 100, 500, and 700 mbar). Scale bar = 500 μm. g) Membrane displacement as a function of the applied pressure (previous design in orange and upgraded design in blue). h) Strain (%) applied to the hydrogel in different sections of the cell-hydrogel chamber using the same pressure range (100–700 mbar).

the device. As previously described,[17] the agarose hydrogel was not covalently attached to the PDMS. After 1 minute, chondrocyte proliferation medium was added to the perfusion channel. Three different sets of culture conditions were tested: (i) static, with no mechanical stimulation; (ii) compression only (300 mbar applied pressure, at 1 Hz to roughly emulate the pace of walking) (Video S1†); and (iii) multi-directional mechanical stimulation (Video S2†), using a unique sequence of compression and shear strain (applied stimulation: 300 mbar positive pressure, −350 mbar negative pressure, frequency of 0.33 Hz, see Video S2 and Fig. S1†). Mechanical stimulation was applied from day 1 in the device, for 1 h per day. All actuation modalities were applied using a dedicated set-up comprising a positive pressure controller, a negative pressure source, a set of 2 way valves (2-switch, Fluigent) allowing rapid pressure switching and AiO software, as previously reported.[17] To enhance matrix formation after the first day of culture, medium was changed from chondrocyte proliferation medium to chondrocyte differentiation medium (DMEM with 1× insulin–transferrin–selenium (ITS)-premix, 100 U ml^{-1} penicillin and 100 μg ml^{-1} streptomycin, 4 mM proline, 50 μg ml^{-1} ascorbic acid 2-phosphate, 1× sodium pyruvate, 20 ng ml^{-1} TGF-β3, 10^{-7} M dexamethasone). Medium was changed daily in the devices.

Chondrocyte deformation in the cartilage-on-chip

Cell deformation was quantified after exposure to mechanical stimulation in the cartilage-on-chip device on day 1. Specifically, the hydrogel section was divided in 3 different zones to account for the gradient in mechanical forces across the hydrogel, from the membrane to the separation pillars, of the same width (400 μm): one close to the actuation membrane (top zone); one close to the pillars (bottom zone); and one in between (middle zone). Images of 30 individual cells (10 for each zone) were acquired with a 40× objective using an inverted microscope (IX51, Olympus, Japan) equipped with a camera (ORCA-flash 4.0 LT, Hamamatsu Photonics, Japan), and the projected surface area of each cell determined for various compression levels (from 0 to 700 mbar – applied pressure) (Fig. 2). Image analysis was performed as previously described.[17]

Analysis of cytokine production using SPRi measurements

Cytokine production was quantified using an in-house nanoparticle enhanced surface plasmon resonance imaging (SPRi) approach.[21] Specifically, antibodies for IL-6 (cAb clone MQ2-13A5), IL-1β (cAb clone JK1B1) or TNF-α (cAb clone Mab1, all Biolegend, San Diego, CA, USA) were immobilized on G-type

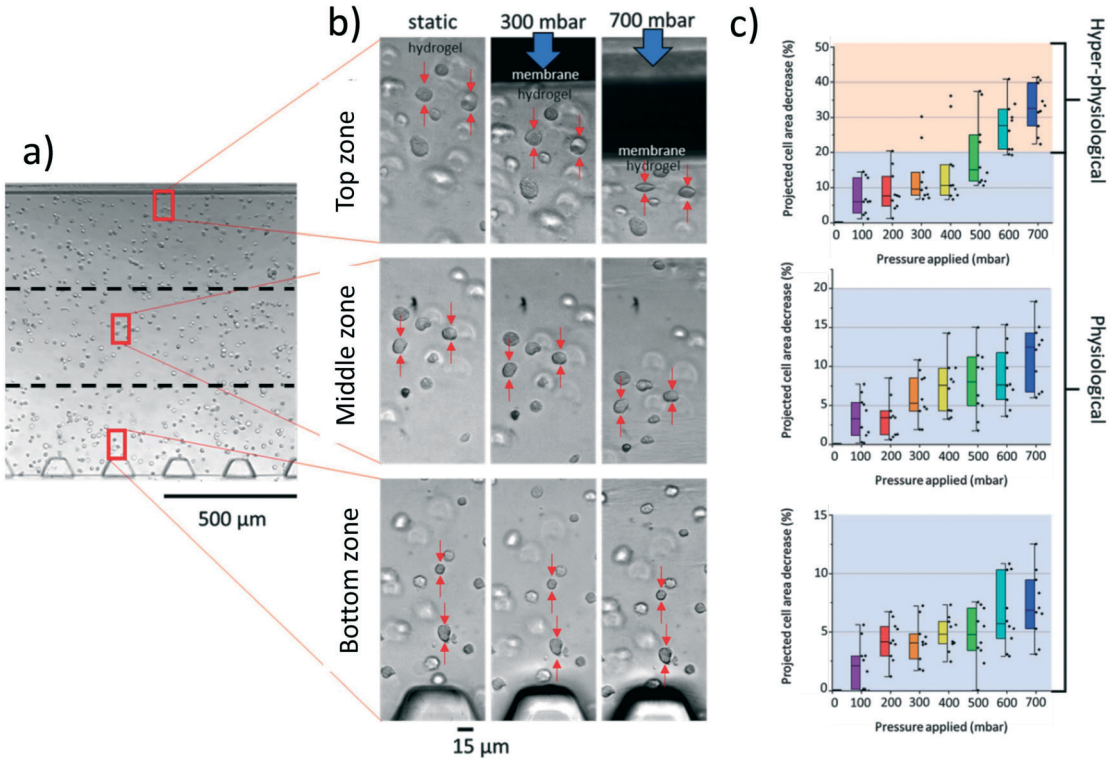

Fig. 2 Real-time visualization of chondrocyte deformation in the cartilage-on-chip device. a) Top view of the cell culture chamber in the device with human chondrocytes embedded in agarose at rest. b) Top view of the three areas defined in the cell culture chamber for analysis: top zone in proximity to the membrane, middle zone, and bottom zone, close to the pillar array at rest and upon application of compression (300 & 700 mbar). c) Projected cell area decrease measured for ten cells in each zone as defined in b, as a function of the applied pressure (0–700 mbar). The light orange area corresponds to hyper-physiological conditions, and the light blue area to physiological conditions. Note that the scale for the deformation range is different for the three different graphs in c).

easy2spot sensors (Ssens, Hengelo, The Netherlands). These sensors present activated carboxylic groups on their surface that readily react to free amines on the antibodies, to covalently immobilize them. The immobilization was performed by manually applying a 300 μl drop of antibody solution on the sensor followed by 30 min incubation. The reaction was performed using a 10 μg ml^{-1} antibody solution in a 10 mM acetic acid buffer (pH 4.6). To reduce non-specific interactions, the sensor was deactivated with 1% BSA in 10 mM acetate buffer at pH 4.6 for 10 min, followed by 0.1 M ethanolamine at pH 8.5 for an additional 10 min.

Medium samples were collected at day 1, 2, 3, 5 and 7 from the perfusion channel of at least three cartilage-on-chip platforms per time point (n = 3, ~2–3 μl per device). The medium samples (60× diluted in PBS with 0.075% Tween80 and 0.5% BSA) were incubated on antibody-functionalized sensors using the Wasatch microfluidic continuous flow spotter (Wasatch Microfluidics, Salt Lake City, UT, USA) for 120 min. Thereafter, the sensors were placed in the IBIS MX96™ (IBIS Technologies, Enschede, the Netherlands) for SPRi measurements. Measurements were programmed using dedicated SUIT software (IBIS Technologies) by setting the type of interaction, interaction times, samples, and regions of interest (ROIs) for the medium samples. Subsequently, a template was created and loaded into the IBIS data acquisition software. Before each experiment an angle offset was applied to ensure a wide dynamic detection range. After programming, the machine provides automatic liquid handling and SPR angle measurements. Back-and-forth flow was set to 10 μl min^{-1} in a flow cell containing 12 μl of sample. An SPRi signal enhancement cascade measurement was performed to achieve desired sensitivity. First, an interaction was performed with the specific detection antibodies for IL-6 (dAb clone MQ2-39C3, Biolegend), IL-1β (dAb clone JK-1B2, Biolegend) or TNF-α (dAb clone Mab11, Biolegend) for 30 min at 2.5 μg ml^{-1} (IL-6) or 5 μg ml^{-1} (IL-1β or TNF-α). Subsequently, neutravidin was injected at 15 μg ml^{-1} (25 nM) for 15 min followed by biotinylated gold nanoparticle at 77.69 mg ml^{-1} (0.2 nM) for another 15 min. Each step in the cascade increases the interaction signal and thus the sensitivity of the assay. The entire amplification cascade increases the signal by a factor 200 and the sensitivity by a factor 40 000.[21] For each experiment, 48 sensor spots were used containing the medium samples. Sprint software was used for data collection and referencing. Data were subsequently exported to Matlab R2015a for further analysis and quality control using custom scripts (available upon request[22]).

Gene expression analysis

After 7 days of culture in the cartilage-on-chip platform, using either culture settings, the agarose hydrogel was retrieved from the device after peeling off the microfluidic layer. For gene analysis, to collect enough mRNA, three independent devices were pooled, which was considered as one sample. Total RNA was extracted using RNeasy Micro Kit (cat. number 74004, QIAGEN, Hilden, Germany) following the protocol described by the supplier. Next cDNA was synthesized using the iScript™ cDNA Synthesis Kit (Bio-Rad, Hercules, CA, USA). The resulting cDNA was subjected to qPCR using SensiMix™ SYBR® & Fluorescein Kit (Bioline, London, UK) on a CFX Connect Real-Time System (Bio-Rad). The following primers were used: *GAPDH* forward 5′-CGCTCT CTGCTCCTGTT and reverse 5′-CCATGGTGTCTGAGCGATGT; *SOX9* forward 5′-TGGGCAAGCTCTGGAGACTTC and reverse 5′-ATCCGGGTGGTCCTTCTTGTG; *COL10A1* forward 5′-GCAA CTAAGGGCCTCAATGG and reverse 5′-CTCAGGCATGACTGCT TGAC; *COL2A1* forward 5′-CCAGATGACCTTCCTACGCC and reverse 5′-TTCAGGGCAGTGTACGTGAAC; *COL1A1* forward 5′-GTCACCCACCGACCAAGAAACC and reverse 5′-AAGTCCAGG CTGTCCAGGGATG. All gene expression level values were normalized to *GAPDH* and are presented as $2^{-\Delta\Delta Ct}$. *GAPDH* expression was checked to be stable for all the different samples (data not shown).

Histological analysis – glycosaminoglycan (GAG) expression

To assess glycosaminoglycan (GAG) production, samples retrieved from the cartilage-on-a-chip devices were fixed, washed with PBS, embedded in Cryomatrix™ (Thermo Fisher Scientific, Waltham, MA, USA) and cut into 10 μm thick sections with a cryotome (Shandon, Thermo Fisher Scientific). Sections were next stained with Alcian blue 8GX (CI 74240) for proteoglycan and counter-stained with nuclear fast red for the chondrocyte nuclei. Four culture conditions were included in this analysis: static culture (at day 0 and day 15), compression only and multi-directional mechanical stimulation using the same procedure as described in section 2.4 (with stimulation starting at day 1 and one final day at rest; 15 days of on-chip culture in total). The pericellular matrix layer thickness was measured for 40 individual cells regardless their position in the hydrogel, for each condition using ImageJ (NIH, Bethesda, MD, USA). Next, to determine whether there was a difference in pericellular matrix formation depending on the type of the applied stimuli, samples, for compression only and multi-directional stimulation, were divided in 6 zones, each of 200 μm in width. Noteworthy, the 260 μm wide zone close to the pillar array was not considered in this analysis, since we observed significant deformation of the hydrogel against and between the pillars. For each zone, both the pericellular matrix thickness and the cell diameter were quantified. To determine the overall GAG production, ten independent zones, at random locations in the hydrogel were considered and the gray intensity value quantified in these areas, the higher the grey value, the higher the GAG production. Background noise was eliminated, and intensity values normalized.

Viability assay

Cell viability was assessed for both static (day 1 and day 7) and compression only culture (day 7) using calcein AM (green/live) and ethidium homodimer-1 (red/dead) (Thermo

Fisher Scientific). The viability percentage was calculated as follows:

$$\text{viable cells (\%)} = \frac{\text{green cells}}{(\text{green cells} + \text{red cells})}$$

For each condition, three individual cartilage-on-chip devices were considered and all cells in the entire chamber imaged using an EVOS FL microscope (Thermo Fisher Scientific).

Immunofluorescence and ECM production

To determine whether the exact mechanical stimulation modality would influence the production of key hyaline cartilage ECM proteins, on-chip samples were cultured for 14 days with exposure or not to mechanical stimulation. In this set of experiments, culture was first static for 7 days, followed by 7 days of mechanical stimuli (compression or multi-directional mechanical stimulation) with the same parameters as before. Devices were disassembled, and samples washed with PBS and fixed in 4% buffered formaldehyde solution. Fixed samples were washed twice with PBS and permeabilized with 0.25% Triton X-100 in PBS for 30 min, washed again with PBS and blocked with a 1% bovine serum albumin solution in PBS for 1 h (all at room temperature). Next, the primary antibody was incubated overnight at 4 °C. After washing with PBS three times the secondary antibody was incubated for 1 h with the samples followed by washing. Lastly, DAPI (4′,6-diamidino-2-phenylindole, 1 : 500 dilution rate) was added for 15 min and three final washes were performed with PBS. The primary antibodies were ACAN (anti-aggrecan antibody [6-B-4] (ab3778), Abcam, Cambridge, UK), COL2 (collagen II antibody (ab34712), Abcam) and COL6 (anti-collagen VI antibody (ab182744), Abcam). The secondary antibodies used were Alexa fluor 647 anti-mouse (ab150107, Abcam) and Alexa Fluor 488 anti-rabbit (A-11008, Invitrogen). Images were taken with a NIKON Eclipse TI confocal microscope (NIKON, Tokyo, Japan). The presence of pericellular proteins was determined by looking at 40 independent chondrocytes for each condition (static, compression only, multi-directional mechanical stimuli). A cell was considered as expressing proteins when a crown or partial crown of proteins was detected. Cells in the 3 zones (top, middle & bottom) were considered; yet all were selected in from of the middle actuation chamber to rule out any inhomogeneity issue.

Statistical analysis

Statistical analysis was conducted using ORIGIN2019 and Tukey one-way ANOVA test.

Results

Cartilage-on-chip device to exert multi-directional mechanical stimulation on a 3D human chondrocyte-laden matrix

Briefly, our cartilage-on-chip platform comprises a cell culture chamber, sandwiched between a perfusion channel and a mechanical actuation unit. The actuation unit consists of a 50 μm thick PDMS membrane actuated by three individually addressable chambers connected with each other through a 50 μm space. The chamber for the cell-hydrogel construct is flanked on one side by the PDMS membrane, whose deflection results in the application of mechanical stimulation onto the cells, and on the other side by an array of pillars to contain the hydrogel matrix, while supporting the delivery of nutrients to the cell-hydrogel construct (Fig. 1a–c). The design was modified from our initial version. First, to improve the device performance in terms of membrane deformation with respect to the applied pressure, the membrane height was increased to 250 μm compared to 220 μm in the previous design, for the same membrane thickness (50 μm). This change in membrane dimensions brought two main additional benefits: the applied pressure was easier to control with lower fluctuations, and less device failure was observed. As before, a 20 : 1 PDMS ratio was employed to maximize the membrane deformability while ensuring the device structural integrity. Next, the pillar cross-section was changed from a square[17] to a trapezoid, to increase the surface tension and better contain the hydrogel in the culture chamber (Fig. S2†).

We first thoroughly characterized this new design in terms of membrane displacement and hydrogel deformation to confirm its enhanced performance, for various applied pressures (compressive forces only). First, the membrane displacement was quantified for the two designs for up to 1200 mbar applied pressure in all actuation chambers (Fig. 1f). As expected, the membrane displacement in the new design was significantly greater for the same applied pressures (Fig. 1g). Even at the highest applied pressure (1200 mbar) the membrane deformation in the initial design remained lower than that achieved using a higher membrane, for a twice lower applied pressure (600 mbar). We also confirmed that different deformation patterns could be created, such as a multi-directional mechanical stimulation (mdms), using a dedicated sequence of positive and negative pressures in the different actuation chambers (Fig. S1 and Video S3†). This mdms pattern, which has been characterized in our previous work, consists of a combination of compressive and shear forces.[17] Both types of forces are greater in the vicinity to the membrane, and progressively decrease across the cell culture chamber in the direction towards the pillars. Additionally, the shear forces were found to be higher at the separation between two actuation chambers, as reported in our previous work.[17] Since our device makes use of three discrete mechanical actuation chambers, the proposed multi-directional mechanical stimulation is reminiscent of a waveform of mechanical stimulation, emulating the rolling motion of two moving cartilage surfaces in a diarthrodial joint.

We next determined the deformation of low melting point agarose inserted in the culture chamber under compression only, at different applied pressures (0–700 mbar), after addition of 15 μm diameter microbeads (Fig. 1h). Low

melting temperature agarose was employed here since it has been reported to support the ECM production of chondrocytes. It has also been vastly used for both static and dynamic *in vitro* models, and for investigating the chondrocyte pericellular matrix.[23–25] The displacement of 47 microbeads was quantified; due to the possible presence of inhomogeneities next to the separation between actuation chambers, these microbeads were considered in front of the middle actuation chamber. Moreover, microbeads that were changing planes upon applying pressure, were excluded from the analysis. This quantitative analysis revealed, as expected, that the closer the microbead to the membrane, the greater its displacement (Fig. S3†). Strain was finally measured, first subdividing the hydrogel chamber in 6 parallel regions, each of 200 μm in width, and measuring, in each section, the average displacement of 5–7 microbeads. This subdivision was chosen to ensure adequate representation of the deformation of the entire hydrogel. It should be noted, that here again, the area close to the array of pillars was omitted in the analysis. The strain profile across the hydrogel chamber fully correlated with the microbead displacement: once more, the higher the applied pressure and the closer to the actuation unit, the higher the strain generated in the hydrogel. Finally, at applied pressures above 500 mbar the strain generated in the hydrogel was higher than 20% reaching values up to 33% in proximity of the membrane (Fig. 1h). To note is the partial spread of microbead displacement which can be potentially explained by the presence of inhomogeneities in the hydrogel structure (Fig. S3†). Agarose is a porous structure with different pores, which translates to possible differences in the dissipation of the forces. Therefore, the recorded deformation is only an approximation of the forces exerted onto the chondrocytes.

Physiological and hyper-physiological stimulation of human chondrocytes in the cartilage-on-chip device

In vivo, human chondrocytes experience a wide range of load-induced deformations ranging from healthy (5–20%) depending on the type and length of the stimuli, to hyper-physiological (>20%), as notably found in OA patients or because of improper movement.[26] We next examined the deformation of human articular chondrocytes embedded in agarose in our cartilage-on-chip device, for increasing applied pressure (0–700 mbar) (Fig. 2a and b). Since the actual stimulation experienced by a cell, depends on its exact position with respect to the actuation membrane, the cell chamber was divided in three zones (Fig. 2b). In each zone, the projected surface area of ten individual chondrocytes was measured at rest and when exposed to homogeneous compression, while increasing the applied pressure (Fig. 2c). For all zones, as expected, the cell surface area deformation (%) increased with the applied pressure. In the top zone, closed to the membrane, at 100 mbar the cell deformation ranged between 2 and 15% (physiological), whereas at 700 mbar in the same zone it reached 22–42% (hyper-physiological) (Fig. 2c). This pressure-dependent cell deformation was less remarkable in the other two zones where only physiological stimulation was observed (0–18% in the middle zone, and 0–12% in the deep zone). Using these quantitative cell deformation values, we estimated the force chondrocytes are exposed to in the device, close to the membrane and next to the pillars (see ESI† S1). Depending on the exact applied pressure, and on the position of the cell across the chamber, these forces range from this text on the same line if possible *ca.* 30 to *ca.* 130 nN, which is very similar to the compressive forces Leipzig *et al.* applied on single chondrocytes to study their ECM production level.[27] Based on these results, for all experiments reported in this paper, a 300 mbar pressure was applied in the actuation chamber, since at this pressure, all cells across the entire hydrogel experience significant deformation (3.5–10% on average) while not being exposed to hyper-physiological stimuli. Furthermore, a 1 Hz frequency was chosen in upcoming experiments, based on previous research[28] and to roughly mimic the walking pace of an individual.

Cytokine release by human chondrocytes in static culture and under exposure to mechanical stimulation

Multiple inflammatory cytokines are released by human chondrocytes when subjected to stress, in the form, for instance, of biochemical signals and biomechanical stimuli. Of note, some of these cytokines, such as IL-6, TNF-α and IL-1β, are well-known for their role in inflammation,[29] and they are highly expressed in diseased conditions such as OA or RA.[30,31] Yet, little is known on the impact mechanical stimulation may have on cytokine production. Thus, we investigated whether chondrocytes embedded in a 3D agarose matrix and exposed to mechanical stimulation would exhibit differences in their cytokine release profile. The production of the three cytokines was analyzed for static culture, compression only and multi-directional mechanical stimulation, at different days. Here, for each cartilage-on-chip device, we were able to retrieve 2–3 μl of medium in the perfusion channel, which was next employed for SPRi analysis using an approach we developed to detect low cytokine levels using a signal amplification cascade and nanoparticles[21] (Fig. 3a). First, the IL-6 level was high for the first two days of culture, in both static culture and samples exposed to multi-directional mechanical stimulation, and significantly decreased over time to become undetectable at day 7 in the static culture samples (Fig. 3b). Still, mechanical stimulation was associated with higher cytokine production, with significant differences at day 3 ($0.05 < P_{value} < 0.1$) and day 7 ($0.001 < P_{value} < 0.01$). These results suggest that the chondrocytes presented a pro-inflammatory response upon their injection in the cartilage-on-chip device in agarose hydrogel and that mechanical actuation exacerbated this response. Previous studies have also reported an increase in IL-6 mRNA expression after application of hydrostatic

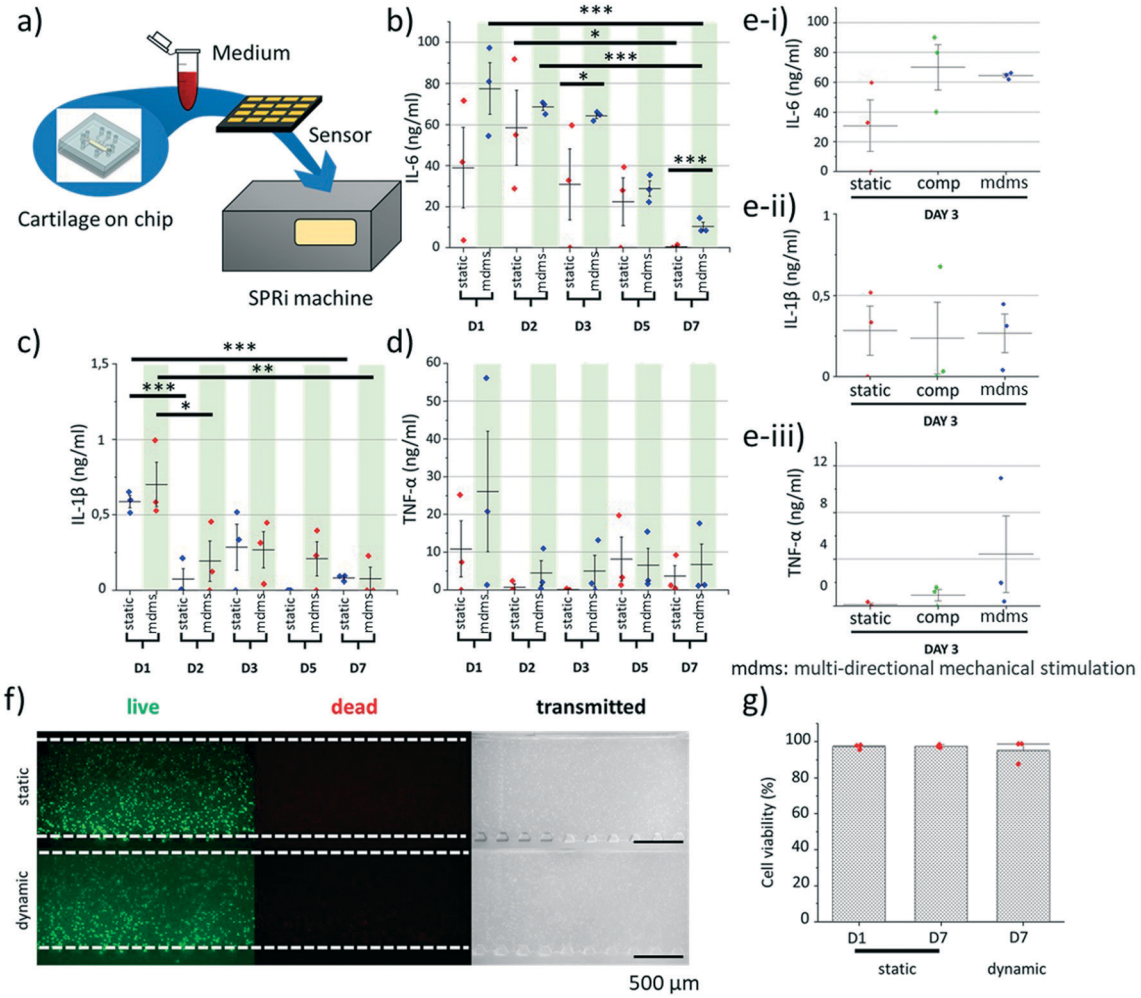

Fig. 3 Cytokine release in the cartilage-on-chip device as a function of time analyzed by SPRi. a) Medium is collected from the devices, diluted before off-line analysis by SPRi. Quantification of the secretion of IL-6 (b), Il-1β (c), and TNF-α (d) in the medium for static culture (red dots) and multi-directional mechanical stimulation (mdms) (blue dots) on different days for 3 independent samples (1 sample = 3 devices). e) Comparison of static culture (red), compression only (green) and multi-directional mechanical stimulation (mdms) at day 3 for IL-6 (i), IL-1β (ii) and TNF-α (iii). f) Cell viability assay using calcein AM (green-live) and ethidium homodimer (red-dead); fluorescence microscopy and corresponding bright-field microscopy images for static and compression only culture. g) Quantification of the viability of human chondrocytes in static (day 1 & 7) and dynamic (compression only, day 7) culture. Scale bar = 500 µm. P_{value}: 0.1 > P_{value} > 0.05*, 0.05 > P_{value} > 0.01**, 0.01 > P_{value} > 0.001***.

pressure on chondrocytes, and chondrocyte monolayers exposed to physiological and hyper-physiological shear stress were found to produce more IL-6.[32,33] Noteworthy, another factor contributing to the small increase in IL-6 level at day 2 could be the change in medium, with a switch from proliferation medium to differentiation medium. It has indeed been reported that some growth factors, such as TGF-β, can trigger inflammation.[34] Nonetheless, over a period of 7 days chondrocytes adapted to their new environment in both conditions, with a remarkable reduction in IL-6 secretion. At day 3, the IL-6 level in the medium was comparable for samples exposed to either compression or multi-directional mechanical stimulation, and higher than for static culture (Fig. 3e-i). This time point was used as a comparison due to the significant difference between static and stimulated samples. A different pattern was observed for TNF-α and IL-1β expression, both over time and between conditions. Their level was initially high on day 1 and significantly decreased from day 2 in culture, this being particularly marked for IL-1β. Still, no statistical difference was found between static and dynamic culture at any day (Fig. 3c and d), and between compression and multi-directional mechanical stimulation (Fig. 3e-ii and iii). Similar results were reported, with a down-regulation of TNF-α and IL-1β in chondrocytes exposed to low mechanical stimulation while hyper-physiological stimulation enhanced their production,[35] and a reduction of IL-1β activity upon exposure to compressive forces.[36,37] To assess whether the high levels of cytokines would be associated with a decrease in cell viability, chondrocytes were stained with calcein AM (green/live) and ethidium homodimer-1 (red/dead) at day 0 and day 7, for static and dynamic (compressive forces only) culture. Of note, cell

viability was not checked for multi-directional mechanical stimulation after the period of 7 days of culture since both mechanical modalities gave similar cytokine release profiles. Cell viability was high in all considered conditions with a slight, but not statistically significant decrease, in the mechanically stimulated samples (Fig. 3f and g). Altogether, the stress response of the chondrocytes after their introduction in the device and exposure to mechanical stimulation did not correlate with any loss in cell viability.

Multi-directional mechanical stimulation promotes the expression of *COL2A1* while inhibiting *COL1A1*

We next evaluated the expression levels of chondrogenic, hypertrophic and proliferation markers for the three culture conditions (static, compression, and multi-directional mechanical stimulation) (Fig. 4b–d). First, the expression level of *SOX9* mRNA was about three times higher after exposure to compression compared to both static culture and multi-directional mechanical stimulation, which both gave similar expression levels (Fig. 4b). This result is in good agreement with previous literature, that reported up-regulation of *SOX9* mRNA expression upon exposure to dynamic compression.[38] Interestingly, both mechanical stimulation modalities resulted in an increase in *COL2A1* and simultaneous decrease in *COL1A1* mRNA expression, compared to static culture. This trend was more pronounced for multi-directional stimulation (*ca.* 1.5- and 2.0-fold decrease for *COL1A1*, and *ca.* 3.0- and 10-fold increase for *COL2A1*, for compression only and multi-directional mechanical stimulation, respectively) (Fig. 4c and d). The mRNA expression of articular cartilage markers *COL2A1* (hyaline), *COL1A1* (fibrotic), *COL10A1* (hypertrophic) and *SOX9* has been previously investigated in other *in vitro* systems with and without mechanical stimulation,[39] yielding contrasting results, most probably due to the difference in the applied mechanical stimulation, type of hydrogel used and length of the stimulation or culture period.[25,40,41] For instance, an increase in *COL2A1* mRNA production has been associated with either an increase in *COL1A1* expression upon exertion compressive forces,[13] or a reduction in *COL1A1* production, when using biaxial stimulation, yet using other hydrogel matrices (gelatin methacryloyl and hyaluronic acid methacrylate) and other loads.[42] The results by us and others suggest that the combination of compression and shear strain further enhances cartilaginous matrix production. We also examined *COL10A1*, a key hypertrophic marker in cartilage, which was not detected in any of the experimental conditions, which can be accounted for by the fact that chondrocytes used in this study were isolated from a healthy donor. At last, mRNA of the proliferation marker *KI67* was not detected, suggesting a non-proliferative phenotype of the chondrocytes, as previously described[17] (Fig. S4†). Altogether,

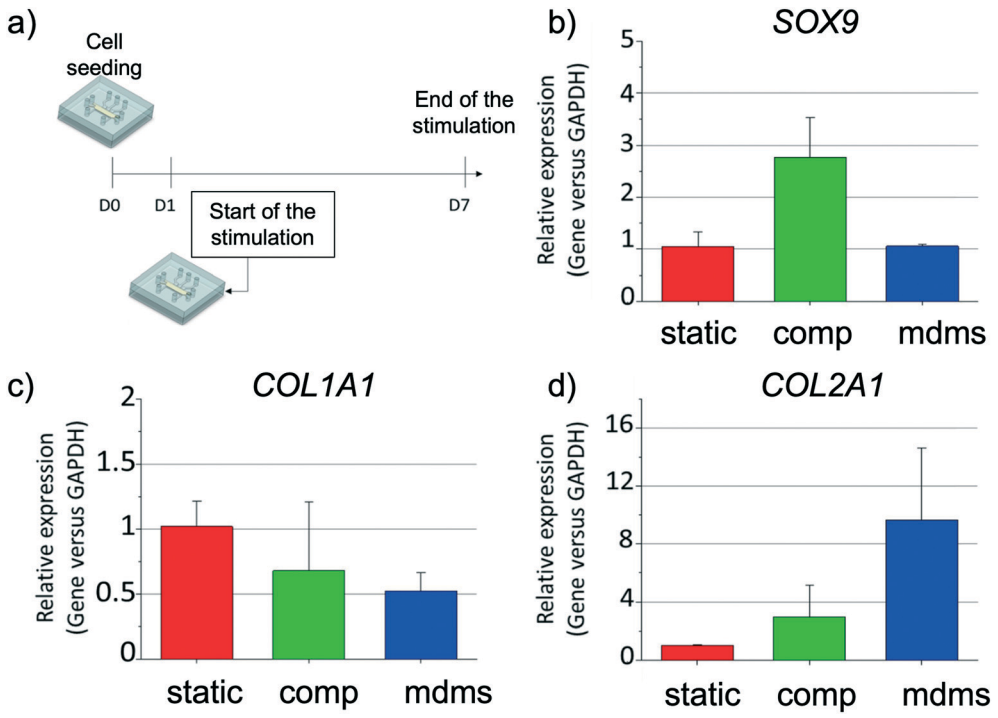

Fig. 4 Gene expression level of chondrocyte markers in the cartilage-on-chip device for static culture, compression only and multi-directional mechanical stimulation (mdms). a) Schematic representation of the experimental design: cells were stimulated every day after one day of culture in the device, for seven days and for 1 h a day, with compression only or multi-directional mechanical stimulation (mdms). Gene expression level of *SOX9* (b), *COL1A1* (c), and *COL2A1* (d) at day 7 in human chondrocytes cultured in static conditions (static, red), under compression only (comp, green) and with multi-directional mechanical stimulation (mdms, blue).

despite the stress initially created by the new on-chip environment mechanical stimulation increased chondrogenic marker gene expression in the cartilage-on-chip model.

Multi-directional mechanical stimulation promotes the formation of both pericellular and interstitial matrices

Chondrocytes in articular cartilage express high levels of glycosaminoglycans (GAGs), which constitute one of the major building blocks of the pericellular and interstitial matrix in the cartilage.[43] Therefore, we examined if mechanical stimulation would have an impact on the GAG production and if this effect would depend on the exact mechanical cues applied to the chondrocyte-laden construct. For this, samples were kept in culture for a longer period,[28] with daily stimulation for 14 days (Fig. 5a). As before, no noticeable cell proliferation was seen, which is in line with the absence of expression of *KI67*, and no cell migration was observed, which allowed us to track individual cells within the agarose matrix over time. Histological evaluation of the retrieved cell-laden hydrogels revealed significant differences in the GAG production upon mechanical stimulation. First, cells cultured under static conditions produced little GAG, with no shell-like structure around individual chondrocytes (Fig. 5b). In contrast, both mechanical stimulation modalities promoted GAG production (Fig. 5b and d): a thin layer of GAG (1 to 5 μm in thickness) was surrounding all chondrocytes, indicating the formation of pericellular matrix after 15 days (Fig. 5b and c and S5†). Remarkably, the thickness of this shell resembles the thickness of the native pericellular matrix in human healthy cartilage.[11,44–48]

We next examined if the location of the chondrocyte in the chamber impacted the pericellular matrix formation, for both stimulation conditions. As expected, the thickness of the shell varied depending on the position of the cells, but, interestingly in a non-monotonous manner. For cells exposed to compression only, this trend was found to have a bell shape (Fig. 5e), with a significantly thicker shell in the middle of the chamber (3.0 ± 0.5 μm) than close to either the membrane (2.0 ± 0.5 μm) ($0.05 > P_{value} > 0.01$**) or the pillars (1.9 ± 0.8 μm) ($0.01 > P_{value} > 0.001$***). This non-monotonous profile could be explained by the presence of the pillars, giving rise to inhomogeneities, and acting as a secondary actuator upon compression of the hydrogel construct against them. In contrast, cells experiencing multi-directional mechanical stimulation gave rise to a slightly different trend, with the highest GAG production found not only in the middle of the chamber (3.2 ± 0.3 μm) but also close to the pillars (3.5 ± 0.8 μm) (Fig. 5e). In the latter area, GAG production was thus significantly more pronounced for the multi-directional mechanical stimulation than for compression ($0.01 > P_{value} > 0.001$***) (Fig. 5e & Table S1†). No significant difference was detected between the two mechanical stimulation conditions for the other sections. Interestingly, these GAG production profiles do not directly correlate with the cell deformation patterns we record for cells in different positions in the device; we believe this can be explained by the differences in experimental conditions. Cell deformation patterns were quantified under static compression at a short time scale, while GAG production was studied after 14 days of stimulation using dynamic loads (1 Hz frequency). Experiments also revealed a difference in cell diameter for mechanically stimulated samples: cells undergoing multi-directional stimulation presented in average a smaller diameter (11.7 ± 1.6 μm) than their counterparts exposed to compression (13.2 ± 1.7 μm). Yet, no clear correlation was found between the chondrocyte diameter and the thickness of pericellular matrix (Fig. 5f).

We finally evaluated the deposition of matrix between cells, or so-called interstitial matrix, in the agarose hydrogel in the same samples. After 15 days of culture under static conditions, a low amount of GAG was found in the agarose matrix. In contrast, exposure to mechanical stimulation resulted in a much higher GAG deposition, this being more marked for multi-directional mechanical stimulation (Fig. 5b and d). Here, possible inhomogeneities near the pillars did not impact the GAG distribution across the chamber (see Fig. S6†), which is not surprising since mechanical actuation helps distribute homogeneously the newly produced GAGs across the cell-hydrogel construct. Finally, these results are in line with previous work, that reported an increase in GAG levels over time for chondrocytes cultured in 3D as individual cells,[23,49,50] and/or exposed to compressive forces.[51] Altogether, the applied stimulation is essential not only for the overall production of GAGs but also for their proper organization into the pericellular environment and surrounding matrix.

Mechanical stimulation enhances aggrecan, collagen II and collagen VI deposition around the chondrocytes

Chondrocytes in articular cartilage produce different types of ECM proteins, this being regulated by a strict balance between anabolic and catabolic activity. In particular, the ECM in hyaline cartilage is rich in aggrecan, collagen II and collagen VI.[52–56] Therefore, we next examined the production of these ECM proteins on-chip, as well as their spatial organization around the chondrocytes using immunofluorescence and confocal microscopy. Based on the SPRi results, indicating a return to normal in expression of pro-inflammatory cytokines after 7 days, we decided to culture the cells on chip for 7 days in static condition first, followed by 7 days of culture with either mechanical stimulation (compression or multi-directional mechanical stimulation) or no compression (Fig. 6a). We analyzed 40 independent cells throughout the agarose hydrogel, all in front of the middle actuation chamber, for their production of these three ECM proteins (Fig. 6b). First, and as expected, mechanical stimulation globally enhanced aggrecan, collagen II and collagen VI production with respect to static conditions (Fig. 6c), which is in line with previous work.[28,42,57] Interestingly, the direction of the mechanical

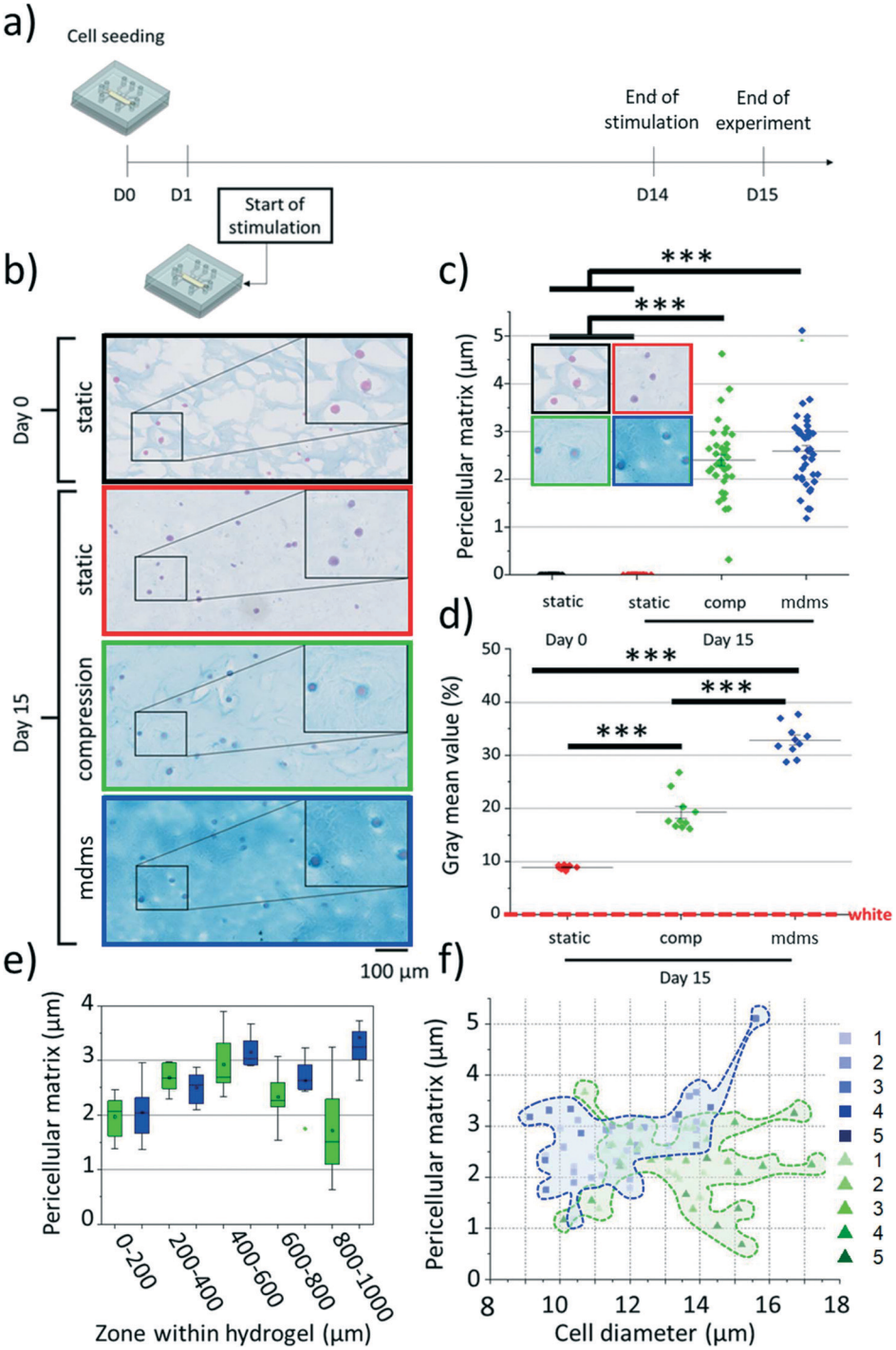

Fig. 5 GAG production by human chondrocytes in the cartilage-on-chip platform. a) Schematic representation of the experimental design; stimulation was applied starting from day 1 until day 14 and samples were fixed the day after. b) Histology section of the chondrocyte-laden agarose for static culture (day 0 & day 15), compression only (day 15), and multi-directional mechanical stimulation (mdms) (day 15). Violet (nuclear fast red) corresponds to cell nuclei and blue (Alcian blue) to GAG. c) Thickness of the formed pericellular matrix shell measured for 40 human chondrocytes in the entire chamber in static culture (day 0 – black, day 15 – red), with compression only (day 15 – blue) and with multi-directional mechanical stimulation (day 15 – green). d) Quantification of the GAG production in the interstitial matrix for each histology section (static – red, compression only – blue, and mdms – green) at day 15. 10 different zones in the hydrogel were considered for this analysis, across the entire chamber. Red intermitted line corresponds to the intensity of the color white in the gray scale. e) Thickness of the pericellular matrix shell for cells exposed to compression only (green) or multi-directional stimulation (blue) in five different zones in the chamber (0–200 µm being close to the actuation membrane), as detailed in the experimental section. In each of the five zones, eight cells were considered. f) Variations in both the chondrocyte diameter and thickness of the pericellular matrix shell for compression only (green) and multi-directional stimulation (blue). As before, eight cells were considered in each of the five zones, and they are represented with a green triangle for compression only and a blue square for multi-directional stimuli (numbers refer to the five zones, starting from the membrane: 1 for 0–200 µm, 2 for 200–400 µm, 3 for 400–600 µm, 4 for 600–800 µm, and 5 for 800–1000 µm). P_{value}: $0.01 > P_{value} > 0.001$***.

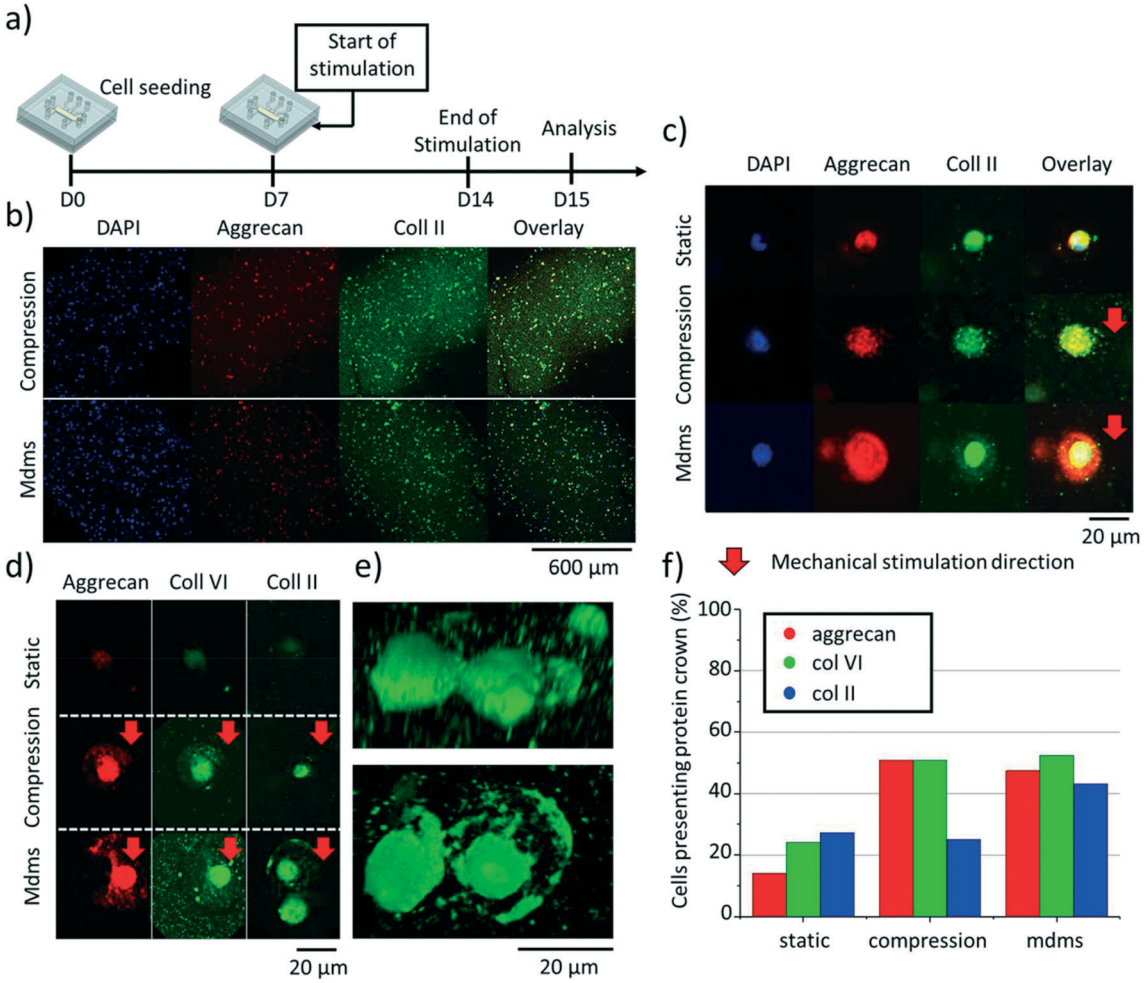

Fig. 6 Chondrocyte production in aggrecan, collagen II and collagen VI after 14 days of on-chip culture. a) Schematic representation of the experimental design; stimulation was applied starting from day 7 until day 14 and fixed the day after. b) Confocal microscopy images of aggrecan (red) and collagen II (green) in agarose section, for both compression only and multi-directional mechanical stimulation (mdms). Nuclei are counter-stained with DAPI (blue). c) Confocal microscopy images of aggrecan (red) and collagen II (green) production of individual human chondrocytes cultured in static, compressive and multi-directional conditions (mdms). Nuclei are counter-stained with DAPI (blue). d) Confocal microscopy images of individual human chondrocytes cultured on-chip, producing aggrecan (red), collagen VI (green) and collagen II (green) in static or dynamic conditions (compression only and multi-directional stimulation (mdms)). e) 3D reconstruction with different perspectives of the collagen II shell (green) for two human chondrocytes exposed to multi-directional mechanical stimulation, shown in d (bottom right picture). f) Percentage of chondrocytes presenting an ECM-based crown or shell structure positive for the three proteins considered here (aggrecan; collagen VI; collagen II).

stimulation impacted the spatial organization of these proteins, whose deposition in the ECM was higher towards the direction of the applied mechanical stimulation (Fig. 6d). Here the ECM proteins were found to form a crown-like structure around individual chondrocytes, which could be a response to protect the cells from mechanical impact (Fig. 6d and e). Aggrecan and collagen VI were similarly expressed in both mechanically stimulated conditions while collagen II production was significantly higher for multi-directional mechanical stimulation than compression only (Fig. 6f). Collectively, these results are in line with the gene expression analysis data (Fig. 4), suggesting that the multi-directional mechanical stimulation on-chip induces the activation of collagen II pathway production in the chondrocytes. Nonetheless, while most of the cells in the agarose matrix produced those proteins, only about half of them were found to exhibit a crown-like structure (Fig. 6f). Furthermore, the increase in pericellular matrix showed by GAG staining along the hydrogel was not detected for these three proteins. These results may suggest a difference in pace in which GAGs and other ECM proteins are produced.

Conclusion

In this work, we assessed the impact of two types of mechanical stimulation on chondrocyte behavior and phenotype in a cartilage-on-chip platform able to deliver a variety of mechanical forces on 3D cell-laden hydrogels, and we overall demonstrated that mechanical stimulation of the

chondrocytes allows emulating the native articular cartilage microenvironment, with a clear advantage of multi-directional mechanical stimuli. First, daily analysis of pro-inflammatory cytokines revealed that the initial seeding of chondrocytes in the agarose matrix in the device induced a stress response, which reverted to normal within one week; we believe this finding is of great interest since it suggests considering a resting period before starting any biological study in our cartilage-on-chip device. Arguably, this finding confirms the well-established knowledge that manipulating cells or exposing them to a different environment can first induce a period of stress. Exertion of physiological mechanical stimulation stimulated the expression of *COL2A1* while simultaneously reducing *COL1A1* expression, leading to the creation of a better cartilage phenotype, especially for multi-directional stimulation. These observations were confirmed at the protein level with the formation of as a quasi-native pericellular matrix shell and significant deposition of GAGs and the hyaline cartilage-related proteins collagen II, collagen VI, and aggrecan around individual chondrocytes to yield chondron-like structures. Altogether, our microscale device allows shaping the mechanical forces exerted on single cells in a cell-hydrogel construct, which is of great interest to screen stimulation conditions and identify optimal mechanical stimulation to tune the ECM protein production by chondrocytes, to emulate the *in vivo* situation.

In the future, it would be of interest to extend this work to include a 3D finite element simulation to have a better understanding on the distribution of the forces across the entire cell-laden hydrogel and correlate this distribution to the cell response depending on their specific location in the device. Next, we intend to study in the future other biomarkers such as MMPs (matrix metalloproteinases), to not only evaluate the production but also the degradation of the ECM components. Next, gene expression analysis was conducted in a global way here, neglecting the influence of the location of the chondrocytes in the device, while immunofluorescence assays did reveal an impact of the chondrocyte-to-membrane distance. In future work, care should be taken to physically cut the hydrogel in bands before mRNA extraction to access this spatial information. Other mechanical stimulation parameters could also be tested, with a different frequency, stimulation, amplitude, *etc.*, also including hyper-physiological cues. In this study, one single healthy donor was considered, while the observed behavior may be donor-dependent; as such, experiments should be repeated with other donors, also considering gender and age differences. Additionally, all experiments were conducted under normoxic conditions, while chondrocytes in cartilage experience a gradient of oxygen between 2 to 6%.[58] This native oxygen gradient can be incorporated, as we recently demonstrated for a tumor-on-chip model.[59] Next, while agarose is acknowledged as a proper matrix for the 3D culture of chondrocytes,[25,40,60] the latter cannot directly bind to this hydrogel. In contrast, other hydrogel materials such as collagen I, hyaluronic acid, and dextran-hyaluronic acid–tyramine hydrogels, support such hydrogel-cell interactions.[61–63] Testing some of these more cartilage-like hydrogels would be interesting in the future, since they are likely to benefit the ECM formation. Still, all in all, our cartilage-on-chip model opens new avenues to conduct basic research on cartilage tissues and for drug testing studies in arthritic diseases, allowing the investigation of multiple parameters with full control on multiple experimental parameters, such as mechanical stimulation and exposure to biochemical stimulation (*i.e.*, drugs).

Conflicts of interest

There are no conflicts of interest to report.

Acknowledgements

This research was funded by the ReumaNederland grant LLP-25.

References

1 X. Houard, M. B. Goldring and F. Berenbaum, *Curr. Rheumatol. Rep.*, 2013, **15**, 375.
2 W. H. Akeson, D. Amiel, M. F. Abel, S. R. Garfin and S. L. Woo, *Clin. Orthop. Relat. Res.*, 1987, 28–37.
3 J. Martel-Pelletier, A. J. Barr, F. M. Cicuttini, P. G. Conaghan, C. Cooper, M. B. Goldring, S. R. Goldring, G. Jones, A. J. Teichtahl and J. P. Pelletier, *Nat. Rev. Dis. Primers*, 2016, **2**, 16072.
4 D. Aletaha and J. S. Smolen, *JAMA, J. Am. Med. Assoc.*, 2018, **320**, 1360–1372.
5 D. Blalock, A. Miller, M. Tilley and J. Wang, *Clin. Med. Insights: Arthritis Musculoskeletal Disord.*, 2015, **8**, 15–23.
6 J. N. Katz, K. R. Arant and R. F. Loeser, *JAMA, J. Am. Med. Assoc.*, 2021, **325**, 568–578.
7 A. J. Sophia Fox, A. Bedi and S. A. Rodeo, *Sports Health*, 2009, **1**, 461–468.
8 G. Musumeci, *J. Funct. Morphol. Kinesiol.*, 2016, **1**(2), 154–161.
9 Z. Zhang, *Tissue Eng., Part B*, 2015, **21**, 267–277.
10 L. G. Alexopoulos, L. A. Setton and F. Guilak, *Acta Biomater.*, 2005, **1**, 317–325.
11 R. E. Wilusz, J. Sanchez-Adams and F. Guilak, *Matrix Biol.*, 2014, **39**, 25–32.
12 L. A. Fortier, J. U. Barker, E. J. Strauss, T. M. McCarrel and B. J. Cole, *Clin. Orthop. Relat. Res.*, 2011, **469**, 2706–2715.
13 P. Occhetta, A. Mainardi, E. Votta, Q. Vallmajo-Martin, M. Ehrbar, I. Martin, A. Barbero and M. Rasponi, *Nat. Biomed. Eng.*, 2019, **3**, 545–557.
14 J. Rosser, B. Bachmann, C. Jordan, I. Ribitsch, E. Haltmayer, S. Gueltekin, S. Junttila, B. Galik, A. Gyenesei, B. Haddadi, M. Harasek, M. Egerbacher, P. Ertl and F. Jenner, *Mater. Today Bio*, 2019, **4**, 100023.
15 D. A. Lee, T. Noguchi, S. P. Frean, P. Lees and D. L. Bader, *Biorheology*, 2000, **37**, 149–161.

16 H. B. Sun, *Ann. N. Y. Acad. Sci.*, 2010, **1211**, 37–50.
17 C. A. Paggi, B. Venzac, M. Karperien, J. C. H. Leijten and S. Le Gac, *Sens. Actuators, B*, 2020, **315**, 127917.
18 L. S. Moreira Teixeira, J. C. Leijten, J. Sobral, R. Jin, A. A. van Apeldoorn, J. Feijen, C. van Blitterswijk, P. J. Dijkstra and M. Karperien, *Eur. Cells Mater.*, 2012, **23**, 387–399.
19 M. Delarue, J. Hartung, C. Schreck, P. Gniewek, L. Hu, S. Herminghaus and O. Hallatschek, *Nat. Phys.*, 2016, **12**, 762–766.
20 E. Delamarche, A. Bernard, H. Schmid, B. Michel and H. Biebuyck, *Science*, 1997, **276**, 779–781.
21 J. Hendriks, I. Stojanovic, R. B. M. Schasfoort, D. B. F. Saris and M. Karperien, *Anal. Chem.*, 2018, **90**, 6563–6571.
22 J. Hendriks, Saving the joint: new methods for early diagnosis and treatment, *PhD thesis*, University of Twente, 2019, DOI: **10.3990/1.9789036548724**.
23 S. Schmidt, F. Abinzano, A. Mensinga, J. Tessmar, J. Groll, J. Malda, R. Levato and T. Blunk, *Int. J. Mol. Sci.*, 2020, **21**, 7071.
24 M. D. Buschmann, Y. A. Gluzband, A. J. Grodzinsky, J. H. Kimura and E. B. Hunziker, *J. Orthop. Res.*, 1992, **10**, 745–758.
25 C. Bougault, E. Aubert-Foucher, A. Paumier, E. Perrier-Groult, L. Huot, D. Hot, M. Duterque-Coquillaud and F. Mallein-Gerin, *PLoS One*, 2012, **7**, e36964.
26 D. L. Bader, D. M. Salter and T. T. Chowdhury, *Arthritis*, 2011, **2011**, 979032.
27 N. D. Leipzig and K. A. Athanasiou, *Biophys. J.*, 2008, **94**, 2412–2422.
28 D. E. Anderson and B. Johnstone, *Front. Bioeng. Biotechnol.*, 2017, **5**, 76.
29 M. J. Pearson, D. Herndler-Brandstetter, M. A. Tariq, T. A. Nicholson, A. M. Philp, H. L. Smith, E. T. Davis, S. W. Jones and J. M. Lord, *Sci. Rep.*, 2017, **7**, 3451.
30 M. Daheshia and J. Q. Yao, *J. Rheumatol.*, 2008, **35**, 2306–2312.
31 J. C. Fernandes, J. Martel-Pelletier and J. P. Pelletier, *Biorheology*, 2002, **39**, 237–246.
32 M. Mohtai, M. K. Gupta, B. Donlon, B. Ellison, J. Cooke, G. Gibbons, D. J. Schurman and R. L. Smith, *J. Orthop. Res.*, 1996, **14**, 67–73.
33 P. Wang, F. Zhu, N. H. Lee and K. Konstantopoulos, *J. Biol. Chem.*, 2010, **285**, 24793–24804.
34 P. A. Guerne, D. A. Carson and M. Lotz, *J. Immunol.*, 1990, **144**, 499–505.
35 J. Deschner, C. R. Hofman, N. P. Piesco and S. Agarwal, *Curr. Opin. Clin. Nutr. Metab. Care*, 2003, **6**, 289–293.
36 T. T. Chowdhury, S. Arghandawi, J. Brand, O. O. Akanji, D. L. Bader, D. M. Salter and D. A. Lee, *Arthritis Res. Ther.*, 2008, **10**, R35.
37 T. T. Chowdhury, R. N. Appleby, D. M. Salter, D. A. Bader and D. A. Lee, *Biomech. Model. Mechanobiol.*, 2006, **5**, 192–201.
38 J. E. Jeon, K. Schrobback, D. W. Hutmacher and T. J. Klein, *Osteoarthr. Cartil.*, 2012, **20**, 906–915.
39 H. J. Samvelyan, D. Hughes, C. Stevens and K. A. Staines, *Calcif. Tissue Int.*, 2021, **109**, 243–256.
40 C. Bougault, A. Paumier, E. Aubert-Foucher and F. Mallein-Gerin, *BMC Biotechnol.*, 2008, **8**, 71.
41 M. D. Buschmann, Y. A. Gluzband, A. J. Grodzinsky and E. B. Hunziker, *J. Cell Sci.*, 1995, **108**(Pt 4), 1497–1508.
42 C. Meinert, K. Schrobback, D. W. Hutmacher and T. J. Klein, *Sci. Rep.*, 2017, **7**, 16997.
43 Q. G. Wang, A. J. El Haj and N. J. Kuiper, *J. Anat.*, 2008, **213**, 266–273.
44 F. Guilak and V. C. Mow, *J. Biomech.*, 2000, **33**, 1663–1673.
45 M. Sancho-Tello, L. Milián, M. Mata Roig, J. J. Martín de Llano and C. Carda, in *Advances in Biomechanics and Tissue Regeneration*, ed. M. H. Doweidar, Academic Press, 2019, pp. 361–378, DOI: **10.1016/B978-0-12-816390-0.00018-2**.
46 G. M. Lee, T. A. Paul, M. Slabaugh and S. S. Kelley, *Osteoarthr. Cartil.*, 2000, **8**, 44–52.
47 E. B. Hunziker, T. M. Quinn and H. J. Hauselmann, *Osteoarthr. Cartil.*, 2002, **10**, 564–572.
48 F. Guilak, R. J. Nims, A. Dicks, C. L. Wu and I. Meulenbelt, *Matrix Biol.*, 2018, **71–72**, 40–50.
49 P. Smeriglio, J. H. Lai, F. Yang and N. Bhutani, *J. Visualized Exp.*, 2015, **104**, 53085.
50 A. K. Kudva, F. P. Luyten and J. Patterson, *J. Mater. Sci.: Mater. Med.*, 2017, **28**, 156.
51 J. D. Kisiday, M. Jin, M. A. DiMicco, B. Kurz and A. J. Grodzinsky, *J. Biomech.*, 2004, **37**, 595–604.
52 L. J. Sandell and T. Aigner, *Arthritis Res.*, 2001, **3**, 107–113.
53 D. Eyre, *Arthritis Res.*, 2002, **4**, 30–35.
54 N. A. Zelenski, H. A. Leddy, J. Sanchez-Adams, J. Zhang, P. Bonaldo, W. Liedtke and F. Guilak, *Arthritis Rheumatol.*, 2015, **67**, 1286–1294.
55 Y. Luo, D. Sinkeviciute, Y. He, M. Karsdal, Y. Henrotin, A. Mobasheri, P. Onnerfjord and A. Bay-Jensen, *Protein Cell*, 2017, **8**, 560–572.
56 P. J. Roughley and J. S. Mort, *J. Exp. Orthop.*, 2014, **1**, 8.
57 S. D. Waldman, C. G. Spiteri, M. D. Grynpas, R. M. Pilliar and R. A. Kandel, *J. Orthop. Res.*, 2003, **21**, 590–596.
58 J. E. Lafont, *Int. J. Exp. Pathol.*, 2010, **91**, 99–106.
59 V. Palacio-Castaneda, L. Kooijman, B. Venzac, W. P. R. Verdurmen and S. Le Gac, *Micromachines*, 2020, **11**, 382.
60 M. A. Dimicco, J. D. Kisiday, H. Gong and A. J. Grodzinsky, *Osteoarthr. Cartil.*, 2007, **15**, 1207–1216.
61 V. Irawan, T. C. Sung, A. Higuchi and T. Ikoma, *Tissue Eng. Regener. Med.*, 2018, **15**, 673–697.
62 R. Jin, L. S. Teixeira, P. J. Dijkstra, C. A. van Blitterswijk, M. Karperien and J. Feijen, *Biomaterials*, 2010, **31**, 3103–3113.
63 R. B. Jakobsen, A. Shandadfar, F. P. Reinholt and J. E. Brinchmann, *Knee Surg. Sports Traumatol. Arthrosc.*, 2010, **18**, 1407–1416.